



Application of spectral signature to analyze quality of magnesite ore mineral deposits and altered rocks of Salem, India

Paramasivam Chellamuthu Ranganathan^{1,2} · Anbazhagan Siddan²

Received: 24 July 2020 / Accepted: 15 March 2021 / Published online: 1 April 2021
© Saudi Society for Geosciences 2021

Abstract

The developers of remote sensing and an advancement of imaging spectroscopy have provided an opportunity to extract compositional information of mineral mixtures. The geochemistry and mineralogical studies support ethical hold on spectral compositional studies of the ultramafic complex. The Salem ultramafic complex region covered by peridotite, dunite, and magnesite ore and surrounded by country rocks like hornblende biotite gneiss and charnockite. The rock samples include peridotite, dunites, metagabbro, and different kinds of magnesite ore minerals collected from the magnesite mines sections and outcrops exposure of reflectance spectral studies, geochemical analysis, and petrographical studies. Spectral measurements were carried out under 350–2500 nm spectral range from whole rock as well as powdered samples of different grain sizes using ASD Spectroradiometer. In the spectral analysis, the intensity of the carbonate bands assumed as fewer than three spectral ranges at 1900 nm, 2300 nm, and 2450 nm bandwidth and band depth based on absorbing characters and quality. The common absorption bands for dunites are 640 nm, 1050 nm, 1392 nm, 1910 nm, 2325 nm, and 2388 nm. In the shorter wavelength region, OH/Mn³⁺, OH/Fe²⁺, Mg-OH vibration and carbonate absorptions indicate the presence of ferric iron, olivine, and pyroxene overlapping spectra. Assessing the proportions of composition of rocks and ore minerals based on the spectral signature is a challenging task due to the minerals that exist in the form of intimate mixtures and variations. A thin section study reveals the presence of the major minerals in the rocks and the characteristics of ore minerals. The XRF geochemistry exposes major oxides and determines correlation of the geochemical elements using cluster and PCA analysis.

Keywords Spectral studies · Ore minerals · XRF · Ultramafic rocks · PCA

Introduction

Spectroscopy is the study of light as a function of wavelength that has been emitted, reflected, or scattered from a solid, liquid, or gas. It is the interaction between matter and electromagnetic radiation (Clark 1999; Gupta 2005). Spectroscopic data are often represented by a spectrum, a plot of the response of interest as a function of wavelength or frequency (Gupta

2005). Spectra may be obtained from the rocks and mineral samples in any of the forms such as whole rocks, or powders (Gaffey 1986). The absorption processes and their wavelength dependence allow us to derive information about the chemistry from its reflected or emitted light. A modern spectrometer, however, can measure finer details over a broader wavelength range and with greater precision (Clark 1999). The spectral measurements have strengthened the surface mineralogical studies with the aid of spectroradiometric principles (Chung et al. 2020). The Spectroradiometer supported for measuring reflectance spectra both in the field and laboratory condition and it is useful to predict diagnostic character of minerals, rocks, certain properties of water bodies, grasslands, forests, crops, and several other surface features from their reflectance spectra (Clark 1999). Lab spectral measurements were carried out from different rocks such as peridotite, dunite, weathered dunite, partially altered dunite, metagabbro, siliceous iron-rich dunites, and ore minerals.

Van der Meer and De Jong (2003) have explicated spectral reflectance in the visible and near-infrared region offers a

This article is part of the Topical Collection on *Recent advanced techniques in water resources management*

Responsible Editor: Venkatramanan Senapathi

✉ Paramasivam Chellamuthu Ranganathan
pusivam@gmail.com

¹ Department of Surveying Engineering, Bule Hora University, Bule Hora, Ethiopia

² Centre for Geoinformatics and Planetary Studies, Periyar University, Salem, India

rapid and inexpensive technique for determining the mineralogy of samples and obtaining information on chemical composition. Different wall rocks, altered rocks, and ores have their spectral reflectance features, which are very helpful for the exploration of remote sensing data and searching for mineral deposits. After the measurement of spectra of rocks and ores in composition with chemical parameters and put forward better wave bands for distinguishing rocks and ores. It explains the association incidence spectral reflectance features of rocks and minerals and that were correlated with their major chemical composition (Bailin and Xingli 1991).

The reflectance spectra of rocks and minerals have unique absorption characters and it is interpreted diagnostic spectral features in the electromagnetic spectrum and the samples are correlated with the albedo range, absorption shape, absorption centers, and band depth (Anbazhagan and Arivazhagan 2010; Paramasivam 2016). The iron oxide minerals in the oxidized zone were identified using spectral analysis. The spectral outputs are consistent with mineralogical data obtained through petrographical studies (Zadeh et al. 2014).

Absorption band parameters such as the position, depth, width, and asymmetry of the feature have been used to quantitatively estimate the composition of samples from hyperspectral field and laboratory reflectance data. The parameters have also been used to develop mapping methods for the analysis of hyperspectral image data. This technique provides surface mineralogical information using absorption band depth and position asymmetry, and simple linear interpolation technique can be planned from hyperspectral image data. It demonstrated that these absorption bands provide basic information for surface compositional mapping and followed by image analysis approaches and data integration techniques (Clark et al. 1990). The spectra indicates the region that has maximum and minimum percentage of minerals (Madani 2011; Van der Meer and De Jong 2003; Gaffey 1986; Gadsden 1975; Zadeh et al. 2014; Anbazhagan and Arivazhagan 2009; Paramasivam 2016).

Natural rocks consist of several minerals of highly variable composition and structure. This affects the behavior of X-rays highly in complex ways. These effects transform directly into the complexities of interpreting fluorescence radiation and are detected in the XRF spectrometer (Brouwer 2010). The rocks and ore minerals were subjected to analysis of geochemical parameters belonging to the major oxides through XRF method. Once the XRF analysis is performed, principal components analysis (PCA) was carried out to simplify geochemical datasets and allow the interpretation of variance within data sets. Once PCA has been performed, cluster analysis can then be used to determine groupings of samples (Chen et al. 2015; Gazley et al. 2015; Xue et al. 2011).

The light emits electromagnetic vibrations that can measure the optical properties of minerals. These observations are used to identify the mineral and study the unique characters of

mineral groups such as plane polarized and crossed polarized property conditions under the petrological microscope (Verma 2010; Raith et al. 2011; Petruk 2000). Quantitative analysis involves the measurement of these intensities for the unknown rock and then compared with appropriate spectral reflectance (Bailin and Xingli 1991). The spectral ranges commonly used in this study are 0.4 to 1.0 μm wavelength range as VNIR and the 1.0 to 2.5 μm range referred as SWIR (Gupta 2005; Mustard and Pieters 1987).

The main aim of this paper is to study the reflectance characters of ultramafic rocks and magnesite ore minerals. The spectral measurement of the whole rocks and different grade of powdered samples were subjected to spectral analysis observation and thereby confirming the lithology. This paper aids to understand the spectral behavior of ultramafic complex and in addition to supporting the spectral signatures with mineralogical and geochemical analysis.

Geological setting

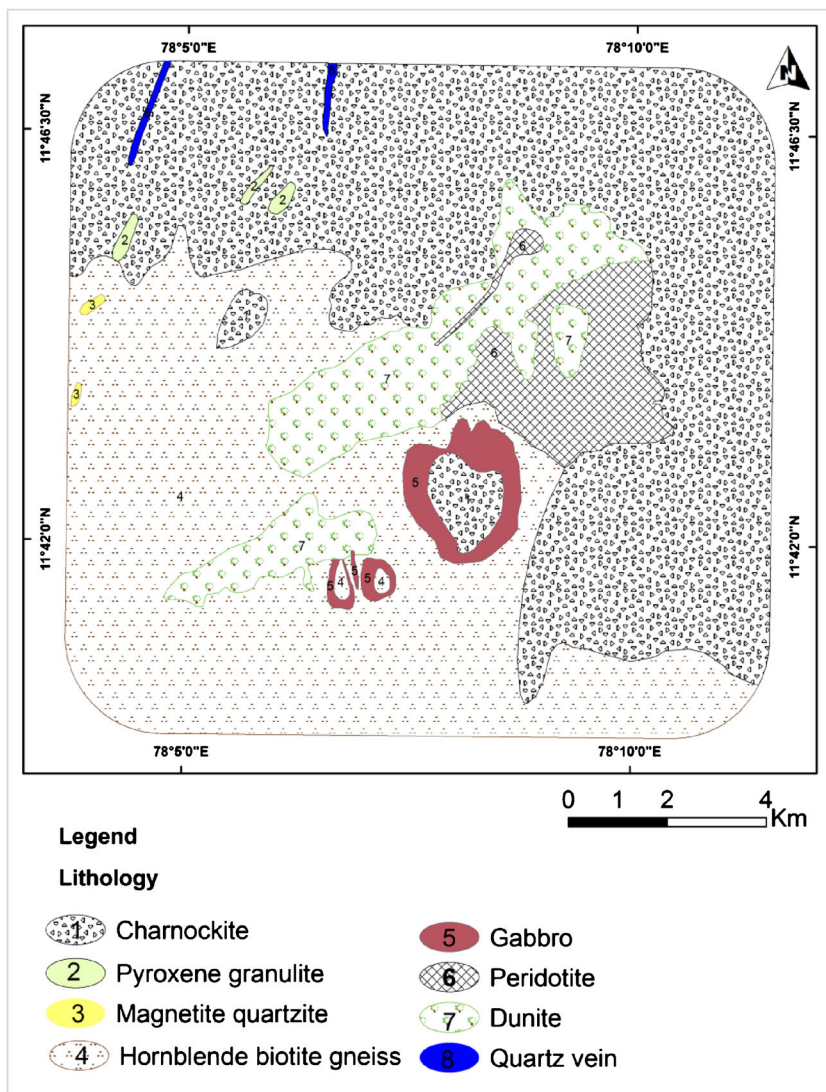
Salem is one of the important locations in the state of Tamil Nadu and known for its geological framework and mineral deposits. The study area covers 190 km^2 under three taluks namely, Omalur, Salem, and Yercaud in Salem district. This is located at the bottom of Shevaroy hills with the longitude between $78^\circ 06' 16''$ E to $78^\circ 19' 25''$ E, and latitude between $11^\circ 66' 47''$ N to $11^\circ 78' 76''$ N. The ultramafic intrusive of chalk hills invaded into pre-existing country rocks of foliated biotite gneiss, migmatite, magnetite, quartzite, eclogite, hornblende gneiss, charnockite, and pegmatites. The ultramafic rocks include Dante and peridotite occurred as intrusive and separated by gneissic rocks (He et al. 2015; Murthy 1979).

The ultramafic intrusion occurred as two intrusive bodies separated by gneisses and granulites and both are disposed in an echelon fashion in an ENE-WSW direction parallel to the general foliation trend of the adjoining gneisses. The larger intrusive occupied in an area of 14.4 km^2 in the northern part. Magnesite formation found as vein type of deposit as fracture filling in dunite and peridotite rocks (GSI 2006; Satish Kumar et al. 2011; Chetty 1996; He et al. 2015; Friend and Janardhan 1984). In chalk hills, magnesite occurs as reticulate, criss-cross and meandering veins of varying thickness. The major part of study area covered by charnockites and gneisses (Fig. 1). Ultramafic rocks generally show evidence of weathering in comparison to the adjacent gneissic rocks (Murthy 1979; Chetty 1996).

Materials and methods

In the present study, an attempt has been made to assess various grades of magnesium ores and rock samples collected

Fig. 1 Geology map of ultramafic terrain– chalk hills, Salem
(Source: GSI, 2006)



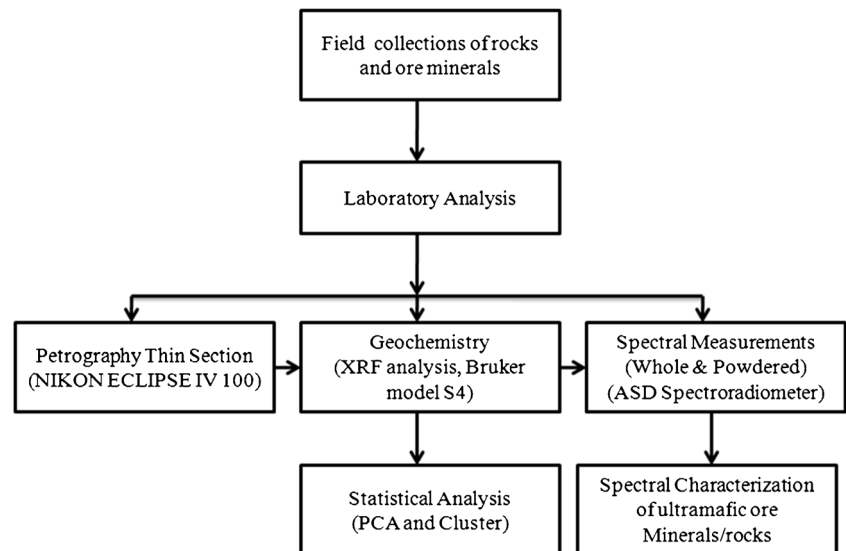
from ultramafic terrain in Salem. There are 12 samples include 6 rock samples and 6 magnesite ore minerals collected from mine sections and outcrop in the ultramafic terrain. The collected samples were partially utilized for chemical analysis and preparation of thin sections for petrographical studies. These samples utilized for preparation of thin sections with specified thickness of 0.03 mm. The thin sections were studied in plane polarized and crossed polarized condition under NIKON ECLIPSE LV 100 polarized microscope for optical properties of minerals.

Spectral measurements were carried out by ASD field Spectroradiometer in the whole rock samples and powdered samples with different grain sizes. The hand specimen has approximate size of 5 cm × 5 cm. In total, 36 rocks (whole rock and pulverized powder samples) and 36 ore mineral samples (whole rocks and powdered samples) were utilized for spectral measurements in the laboratory condition. Powdered

samples were prepared with different particle size as 250–420 μm, 150–250 μm, 105–150 μm, 63–105 μm, and 37–63 μm for spectral measurements. The XRF results are used as input in the STATISTICA (Ver.7) software to perform PCA and cluster analysis. The overview of the methodology adopted in this study is depicted in Fig. 2.

Field sample collection

Magnesite ores occur as veins and an alteration product of ultramafic rocks, serpentinite and other magnesium rich rocks in both contact and regional metamorphism (GSI 2006). Different kinds of magnesite ore minerals (Fig. 3) including high-grade magnesite, medium-grade magnesite, low-grade magnesite, siliceous iron magnesite, magnesite with asbestos, and magnesite gossan were collected in different mines (Table 1).

Fig. 2 Methodology implement in the study

Magnesite mineralization in the ultramafic terrain occurs as fracture filling and vein-lets formation. In fracture filling type, individual veins are parallel or intersecting with each other. In vein-lets type, the veins are relatively thinner from a few millimeters to 10 cm thickness. The peridotite and dunite are exposed at the foothills of the Shevaroy hills. Massive

mineralogical alteration of dunite exhibits serpentine in the first stage and finally transforms into magnesite. Peridotite represents ultramafic rock that contains less than 45% silica and has high proportions of magnesium-rich olivine, with appreciable iron content. Dunite has greater than 90% olivine, with minor amounts of pyroxene and chromite. Different

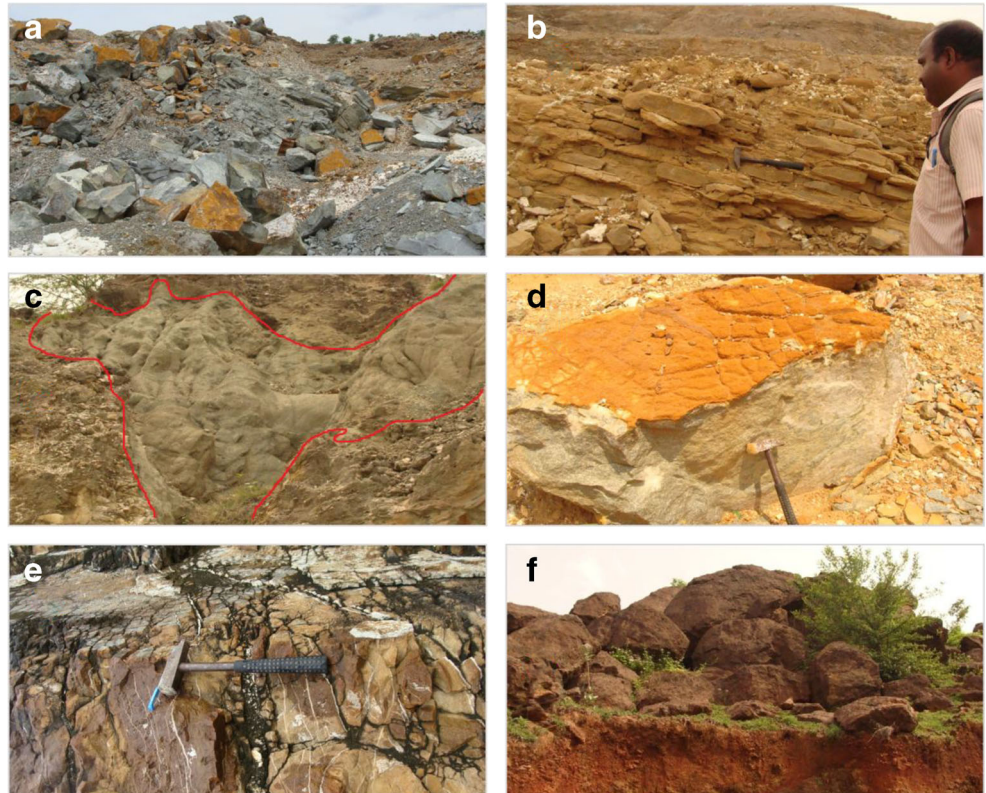
Table 1 Sample locations of ultramafic rocks and ore minerals

Sample ID	Category	Latitude & longitude	Location
SR 6	High grade Magnesite	N 11°41'51.783" & E 78°06'32.720"	SAIL KEEL board mine
TA 4	Medium-grade magnesite	N 11°45'21.996" & E 78°09'33.232"	TANMAG (A-block)
TA 17	Low grade Magnesite	N 11°45'00.204" & E 78°09'04.805"	TANMAG (C-Block top)
DBM 6	Siliceous Iron Magnesite	N 11°43'22.526" & E 78°08'20.476"	Dalmia (MT block)
DBB 21	Magnesite with asbestos	N 11°44'03.830" & E 78°08'32.497"	Dalmia (B- block)
DBM 8	Magnesite outcrop (Gossan)	N 11°43'16.179" & E 78°08'10.592"	Dalmia (Hill top MT block)
SRR 1	Peridotite	N 11°44'48.834" & E 78°08'41.900"	SAIL red hills mine
SR 7	Dunite	N 11°41'51.783"& E 78°06'32.720"	SAIL KEEL board mine
DBA 26	Weathered Dunite	N 11°43'42.978"& E 78°07'55.302"	Dalmia mine A- block
DBM 5	Siliceous iron Dunite	N 11°43'22.526"& E78°08'20.476"	Dalmia mine MT block
SRA 12	Partially altered Dunite	N 11°41'46.011"& E78°06'10.971"	SAIL Abandoned mine
DB 2	Meta gabbro	N 11°43'10.636" & E 78°07'48.971"	Cheetichavadi (adjacent to Dalmia mines)

Fig. 3 Field photographs shown variety of magnesite deposit. (a) magnesite high grade (SR-6), (b) magnesite medium grade (TA-4), (c) magnesite low grade (TA-17), (d) magnesite–siliceous iron (DBM-6), (e) magnesite with asbestos (DBB-21), (f) magnesite (outcrop–gossan) (DBM-8)



Fig. 4 Field photographs shown various ultramafic rock types. (a) peridotite (SRR-1), (b) dunite (SR-7), (c) dunite weathered (DBA-26), (d) dunite siliceous iron (DBM-5), (e) partially altered dunite (SRA-12), (f) meta gabbro (DB-2)



ultramafic rocks such as dunites, weathered dunite, partially altered dunite, siliceous iron dunite, and metagabbro were collected during field investigation (Fig. 4).

Alternating layers of dunite composed of opaque green, greenish-brown country rock mainly occupied by hornblende biotite gneiss in the study area and it primarily occupies about 70 km² areas. Gabbro is a coarse-grained dark plutonic rock consisting of pyroxene, plagioclase feldspar, and often olivine.

Petrological study

The optical properties of magnesite ore minerals and other rocks are studied under the petrological microscope through plane polarized light (PPL) and crossed polarized light (XPL) conditions (Fig. 5). The PPL photomicrograph of high-grade magnesite ore mineral (Fig. 5a) shown as anhedral in shape, cloudy appearance, forming a gel like fracture for altered product of serpentine. The XPL condition shows a low interference color, colorless gray to pale. The magnesite ore has with asbestos (Fig. 5b) in XPL photomicrograph shown low interference color, colorless grey to pale and fibrous appearance. The magnesite gossan type under XPL conditions shows fine texture

and low interference color, colorless grey to pale, very little brownish appearance for Fe content (Fig. 5c).

The peridotite rock sample under PPL condition show interlocking grains of olivine with two sets of cleavage mutually perpendicular to each other moderate to high relief and black color spotted appearance indicates presence of chromite (Fig. 6a). The XPL photomicrograph shows higher order interference colors, straight extinction, strong green color as olivine (OL) yellowish-green, brown, bluish-green in thin section, strong pleochroism and black color spotted appearance indicates presence of chromite (CR).

Dunite in PPL condition shows presence of secondary mineralization along the channels (CH) indicated as signs of fractures (Fig. 6b). In XPL condition olivine shows orange interference colors, grading to violet due to deformation, olivine weathering microtexture in dunite show appearance of blue color (OLW). Dunite with siliceous iron show presence of opaque, moderate to high relief, brownish to reddish black color indication of iron (FE) in PPL conditions (Fig. 6c). The XPL photomicrograph has show strong colored green, yellowish- brown, bluish in thin section. The strong pleochroism and appearance of pink and blue interference colors

Fig. 5 Photomicrograph of varieties of magnesite ore under PPL and XPL conditions (100µm). (a) High-grade magnesite, (b) magnesite with asbestos, (c) magnesite outcrop (gossan)

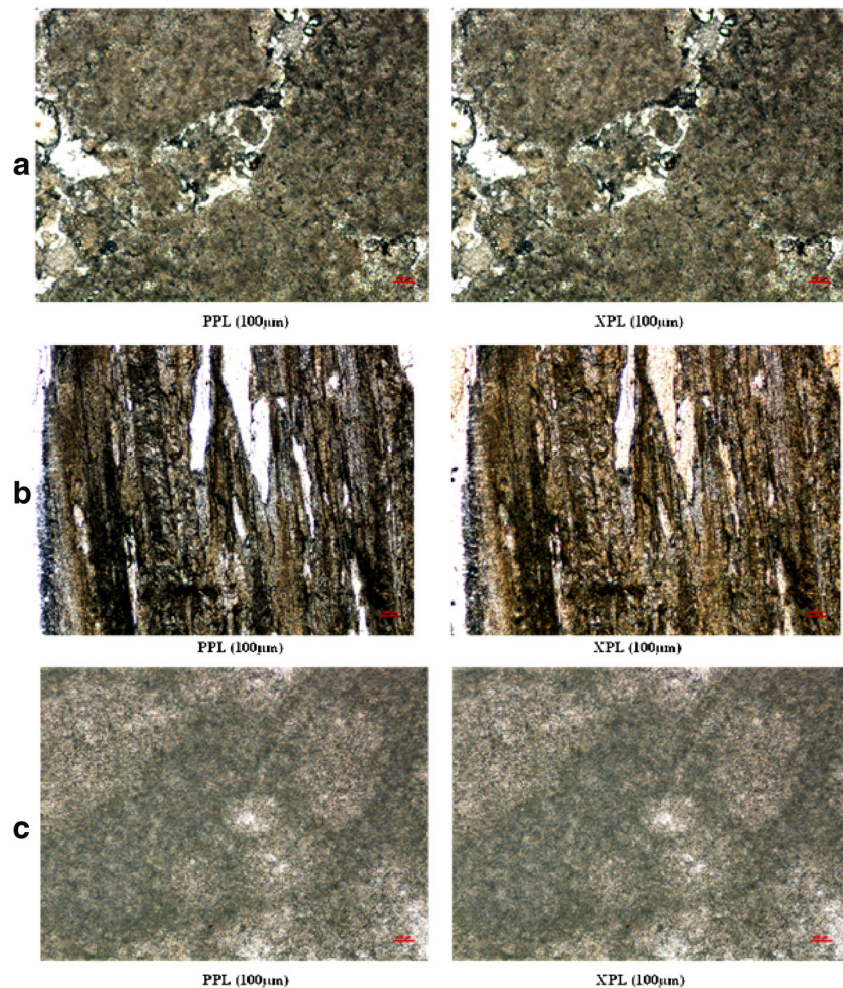


Fig. 6 Photomicrograph of ultramafic rocks under PPL and XPL conditions (100µm) (a) peridotite, (b) dunite, (c) dunite enriched with siliceous iron

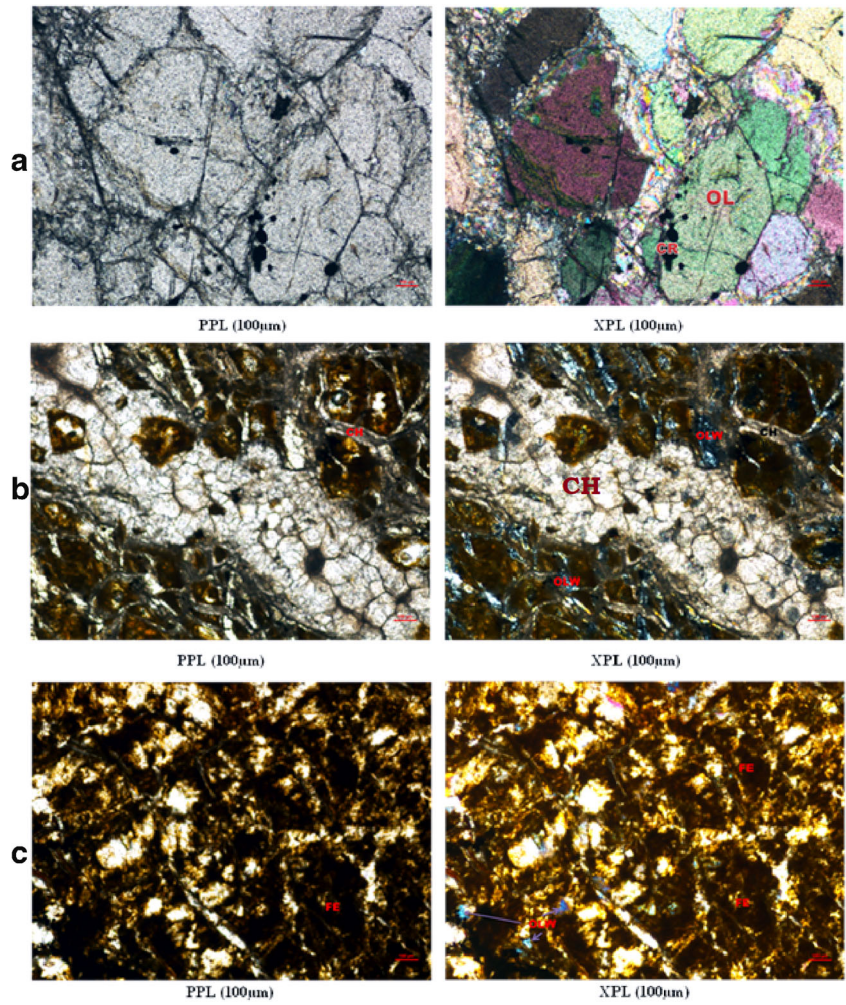


Fig. 7 Photomicrograph of ultramafic rocks under PPL and XPL conditions (100µm) (a) partially altered dunite (b) metagabbro

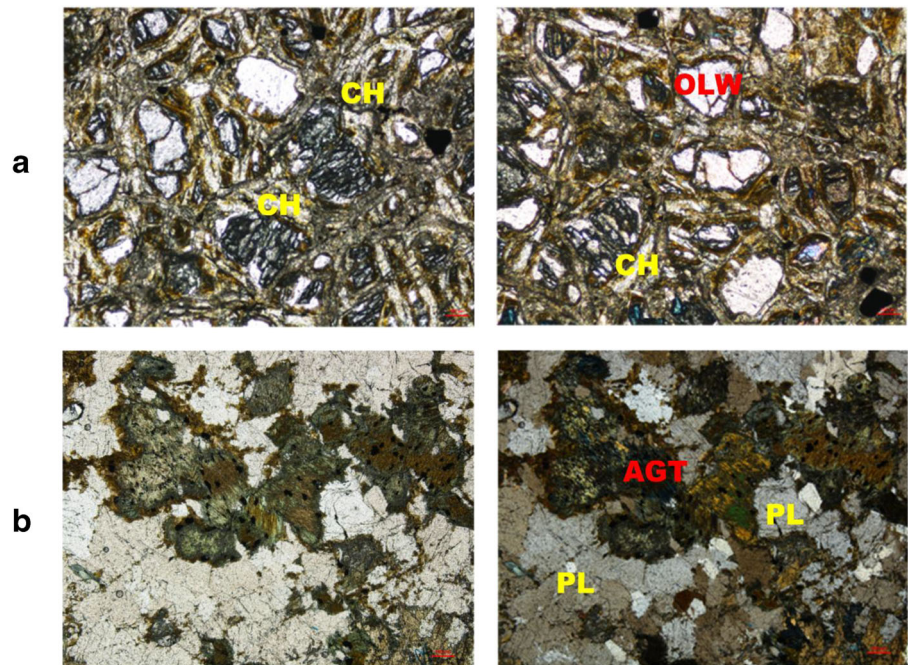


Table 2 Geochemistry of major oxides in magnesite ore minerals and ultramafic rocks

Sample	SiO ₂	TiO ₂	Al ₂ O ₃	MnO	Fe ₂ O ₃	CaO	MgO	Na ₂ O	K ₂ O	P ₂ O ₅	LOI
Magnesite	10.49	ND	0.1	ND	0.1	0.65	41.06	0.1	0.01	ND	47.43
Magnesite with asbestos	22.25	0.02	1.01	0.02	1.06	0.83	35.25	0.05	0.01	ND	39.36
Magnesite gossans	9.70	ND	0.09	0.02	0.74	1.89	41.56	ND	0.01	ND	45.54
Peridotite	36.24	ND	3.55	0.06	5.32	1.35	52.86	0.09	0.02	ND	0.25
Dunite	37.07	ND	0.15	0.08	5.68	0.41	32.5	0.09	0.02	ND	23.65
Weathered Dunite	45.92	0.26	7.58	0.15	9.3	6.08	23.75	0.52	0.35	0.09	5.62
Dunite Siliceous Iron	62.73	0.02	0.3	0.25	18.43	3.21	10.74	0.06	0.03	0.05	4.19
Partially altered Dunite	39.40	0.01	0.21	0.1	6.82	0.69	39.03	0.12	0.02	ND	13.41
Meta gabbro	53.80	0.37	3.31	0.16	10.97	13.58	16.34	0.91	ND	0.08	0.19

ND not determined; LOI loss of ignition

shows as olivine in weathered (OLW) conditions. The partially altered dunite in PPL condition shows the secondary mineralization along the channels and presence of fractures (CH). The olivine mineral shows orange interference colors (Fig. 7a) grading to violet due to deformation, weathering micro texture with appearance of blue and pink color (OLW).

Metagabbro in PPL condition show the presence of large quantity of opaque minerals, pyroxene, and high-relief mineral with visible parallel cleavage (Fig. 7b). Plagioclase show featureless low-relief signature and larger quantity of dark minerals present as pyroxene. In XPL condition, metagabbro show elongate prismatic and subhedral intergranular clinopyroxene augite (AGT) and pale brown color plagioclase (PL) opaque and minor amount of chromite as dark color mineral.

Statistical analysis of geochemistry

The ultramafic rocks and magnesite ore minerals were subjected to XRF analysis for geochemical study with the help of Bruker model S4 Pioneer instrument. The magnesite ore minerals and the rock samples were pulverized into <400 μm

grain size for XRF analysis. The major oxides include SiO₂, TiO₂, Al₂O₃, Fe₂O₃, MnO, MgO, CaO, Na₂O, K₂O and P₂O₅ were analyzed (Table 2).

The Pearson's correlation of geochemical elements in ore minerals magnesite and ultramafic rocks is tabulated in Table 3. The PCA process reduces the complexity in the datasets generated from the collected samples. The PCA significant factors PCA1, PCA2, and PCA3 are calculated for the major oxides (variables) that lies in the linear composition (Chen et al. 2015; Gazley et al. 2015; Xue et al. 2011). The eigenvalue of these principal components is plotted to form a scree plot of major oxides of ore minerals magnesite and ultramafic rocks. The cluster analysis is interpreted through the dendrogram drawn with the linkage distance against the major oxides of the field collected samples (Chung et al. 2016, Chung et al. 2015, Tellen and Yerima 2018).

Spectral measurements

The main objective of the present study is to characterize spectral features of ore minerals and rocks from Salem

Table 3 Pearson's correlation of major oxides ultramafic minerals and rocks

	SiO ₂	TiO ₂	Al ₂ O ₃	MnO	Fe ₂ O ₃	CaO	MgO	Na ₂ O	K ₂ O	P ₂ O ₅	LOI
SiO₂	1.00										
TiO₂	0.49	1.00									
Al₂O₃	0.36	0.70	1.00								
MnO	0.95	0.46	0.29	1.00							
Fe₂O₃	0.95	0.39	0.24	0.99	1.00						
CaO	0.53	0.95	0.52	0.52	0.47	1.00					
MgO	-0.73	-0.58	-0.18	-0.84	-0.80	-0.63	1.00				
Na₂O	0.49	0.98	0.63	0.42	0.37	0.95	-0.53	1.00			
K₂O	0.25	0.45	0.83	0.29	0.22	0.21	-0.25	0.33	1.00		
P₂O₅	0.68	0.88	0.72	0.74	0.67	0.83	-0.78	0.82	0.63	1.00	
LOI	-0.90	-0.51	-0.56	-0.78	-0.79	-0.53	0.41	-0.53	-0.30	-0.61	1.00

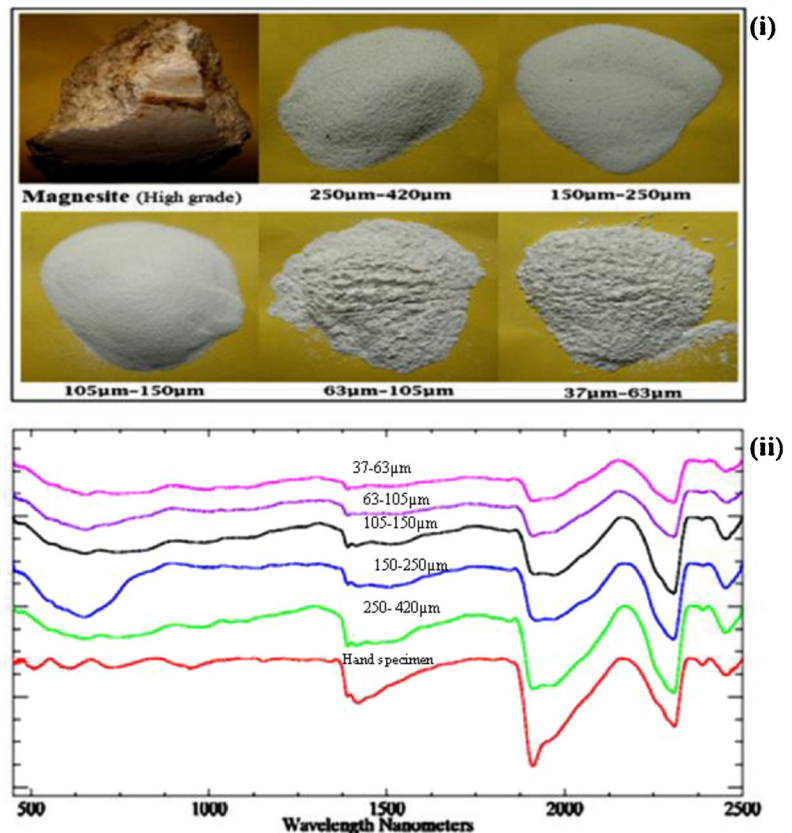
Highly correlated values are in bold



Fig. 8 ASD spectroradiometer used for spectral measurements in laboratory conditions

ultramafic terrain. Spectra may be obtained from the rocks and mineral samples in any of the forms such as whole rocks, or powdered samples. The diagnostics spectral feature is an important parameters were observed from ASD Spectroradiometer for measuring reflectance spectra of rocks and ore minerals (Fig. 8). The instrument attached to standard spectralon, 1' X 1' panel was used as the reference reflectance white plate for calibration and measure 100% reflectance. The whole ore mineral and rock samples and also powdered into different grain sizes 250–420

Fig. 9 Lab spectra for high-grade magnesite ore mineral. (i) Hand specimen and respective powdered samples with different grain sizes (250–420 μm , 150–250 μm , 105–150 μm , 63–105 μm , and 37–63 μm). (ii) Reflectance spectra of high-grade magnesite ore mineral for hand specimen and various grain sizes



μm , 150–250 μm , 105–150 μm , 63–105 μm , and 37–63 μm were utilized to obtain spectra. Spectral data of rocks and ores and physical and chemical parameters in the mathematical statistics are analyzed from the laboratory spectrum data and then grouped to their own characteristics. Spectral measurements were carried out at laboratory for dunites, magnesite ore minerals, and ultramafic rocks in the field collected samples from the magnesite mine section and exposed outcrops.

Result and discussion

Reflectance spectra of magnesite ore minerals

A magnesite ore mineral has crystals of magnesium carbonate, porous masses with dull luster and isomorphous structure. The quality of ore mineral is evaluated based on the percentage of silica content. During field visits, six magnesite ore minerals representing different quality as high, medium and low grade of magnesite, siliceous iron, partially altered, magnesite with asbestos and gossan type magnesite outcrop samples were collected.

The reflectance spectra of magnesite ore minerals in hand specimen and powdered samples show mostly similarity in the spectral signature with minor variations in the albedo and absorption features. The percentage of magnesium and

Fig. 10 Lab spectra for medium-grade magnesite ore mineral. (i) Hand specimen and respective powdered samples with different grain sizes (250–420 μm , 150–250 μm , 105–150 μm , 63–105 μm , and 37–63 μm). (ii) Reflectance spectra of medium-grade magnesite ore mineral for hand specimen and various grain sizes

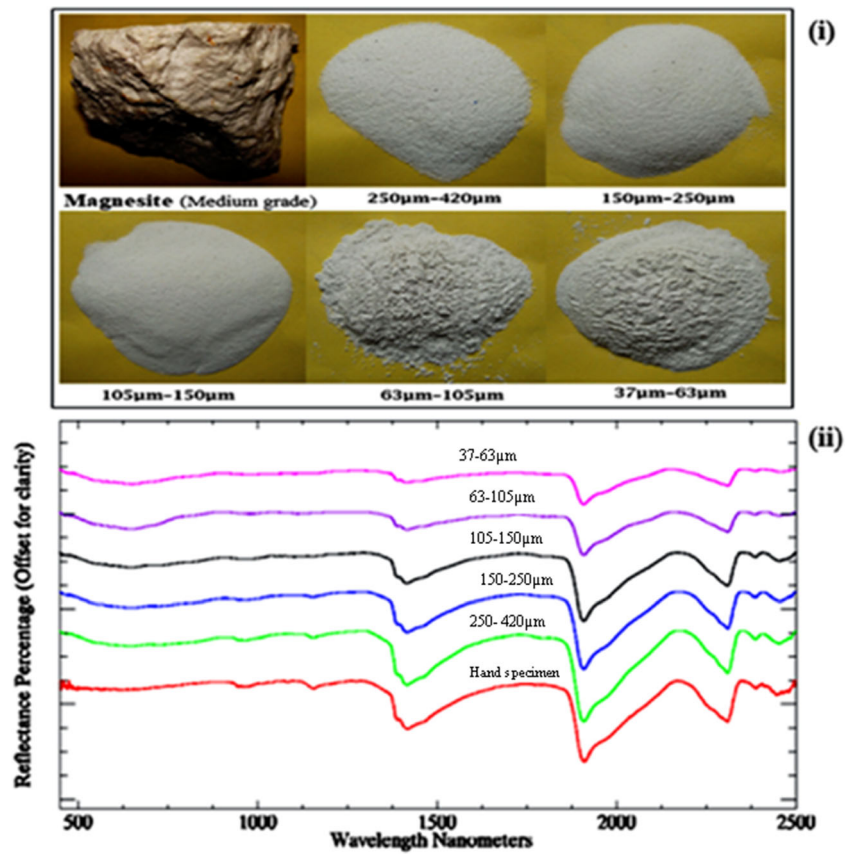


Fig. 11 Lab spectra for low-grade magnesite ore mineral. (i) Hand specimen and respective powdered samples with different grain sizes (250–420 μm , 150–250 μm , 105–150 μm , 63–105 μm , and 37–63 μm). (ii) Reflectance spectra of low-grade magnesite ore mineral for hand specimen and various grain sizes

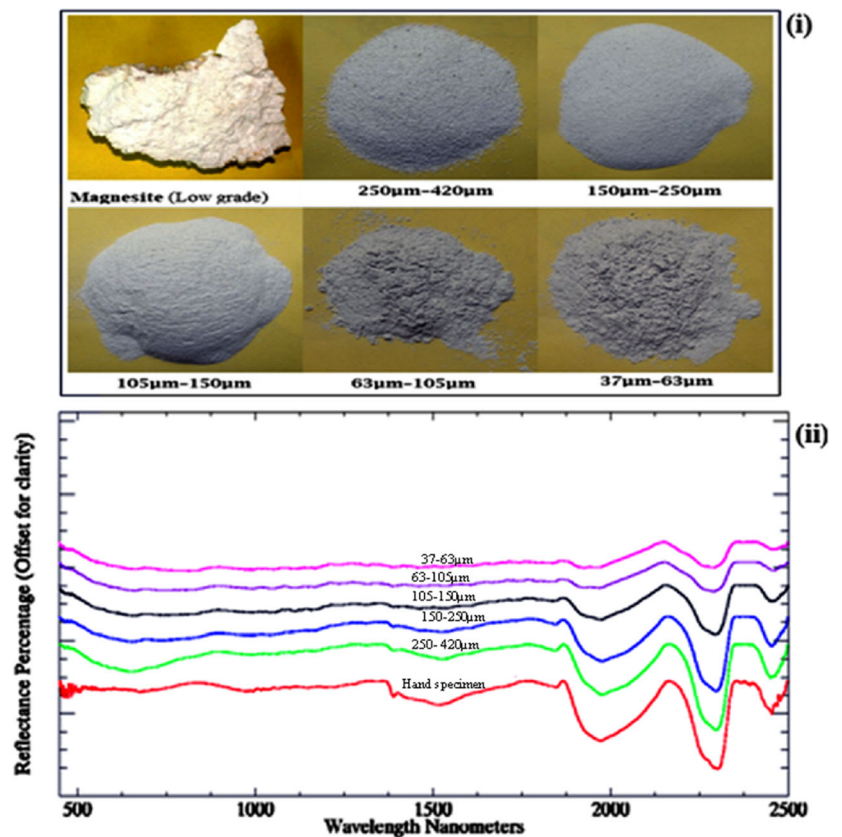


Fig. 12 Lab spectra for siliceous iron magnesite. (i) Hand specimen and respective powdered samples with different grain sizes (250–420 μm , 150–250 μm , 105–150 μm , 63–105 μm , and 37–63 μm). (ii) Reflectance spectra of siliceous iron magnesite for hand specimen and various grain sizes

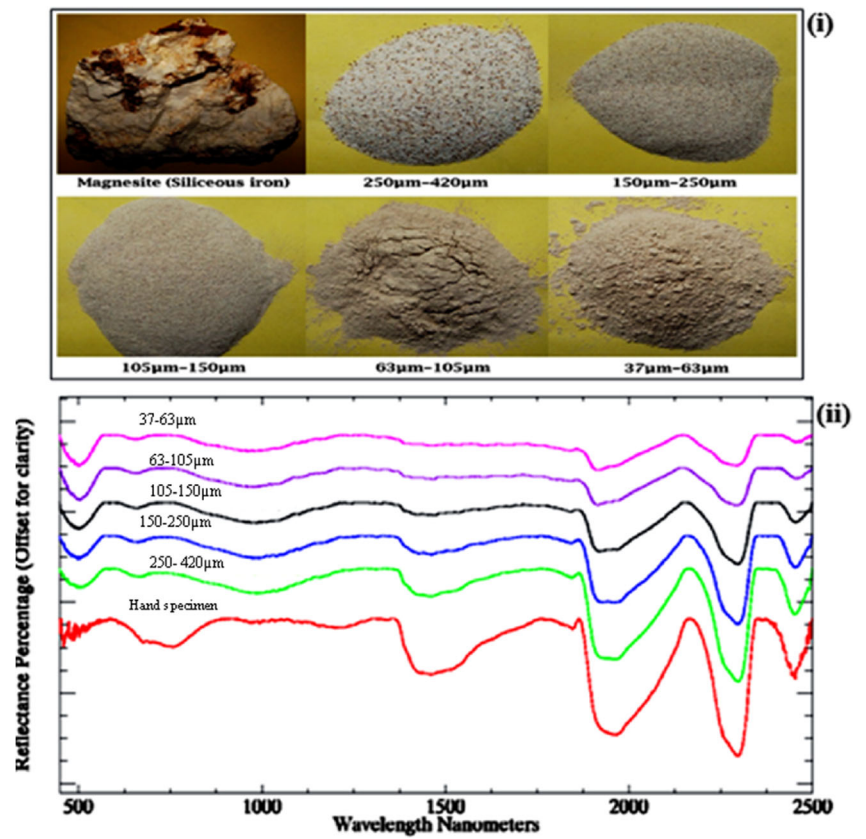


Fig. 13 Lab spectra for magnesite with asbestos. (i) Hand specimen and respective powdered samples with different grain sizes (250–420 μm , 150–250 μm , 105–150 μm , 63–105 μm , and 37–63 μm). (ii) Reflectance spectra of magnesite with asbestos for hand specimen and various grain sizes

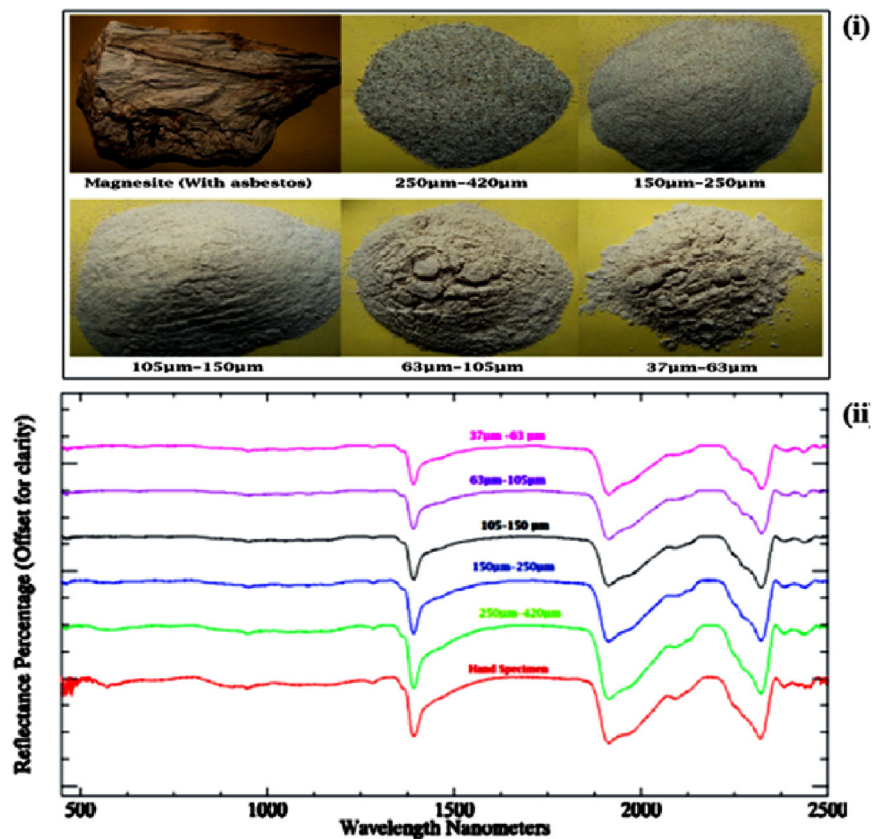
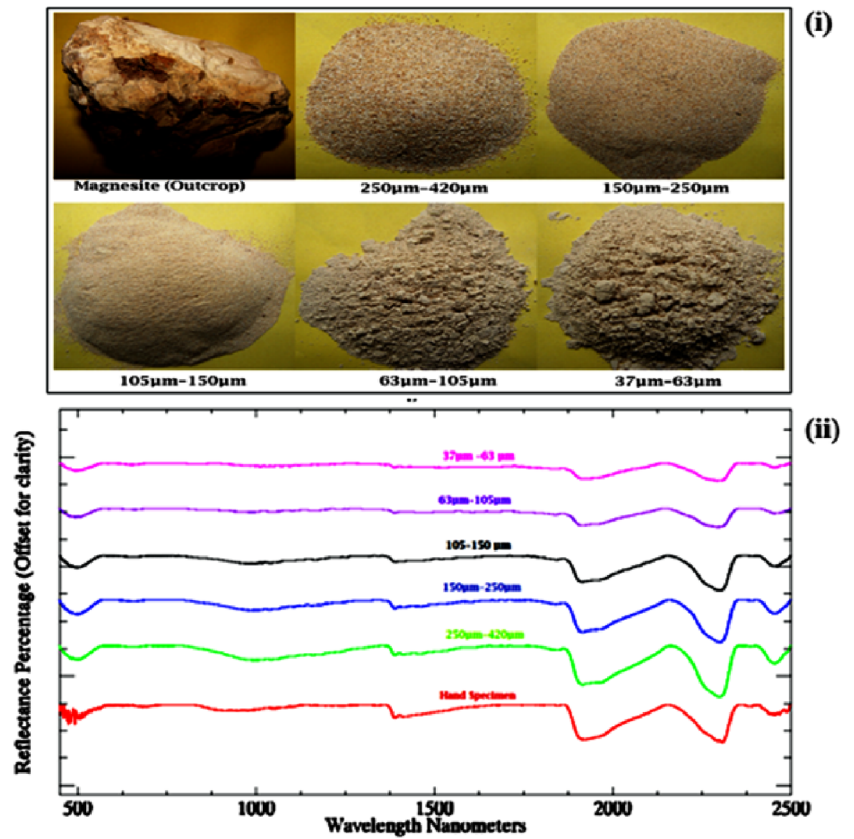


Fig. 14 Lab spectra for magnesite (outcrop) gossan. (i) Hand specimen and respective powdered samples with different grain sizes (250–420 μm , 150–250 μm , 105–150 μm , 63–105 μm , and 37–63 μm). (ii) Reflectance spectra of magnesite (outcrop) gossan for hand specimen and various grain sizes



carbonate influence the absorption feature of magnesite ore minerals. Since is not much absorption features under <500 nm, hence the spectral plot restricted to 500–2500 nm range.

The reflectance spectra of high-grade magnesite show very high albedo ranges from 70 to 96%. It is one of the diagnostic spectral features of magnesite ore mineral. The spectra at 1420 nm and 1916 nm indicate the alteration and presence of hydroxyl ion in the mineral. The combined absorption

signatures at 1916 nm, 2300 nm, and 2457 nm indicate the occurrence of Mg-OH spectral features and trend shows an increase in carbonate and magnesium percentage (Fig. 9). The percentage of reflectance or albedo increases with averages of grain sizes. Similarly, the absorption depth decreases with averages of grain sizes. Strongly absorption noticed in hand specimen and shallow asymmetrical absorption observed in 37–63 μm in grain size.

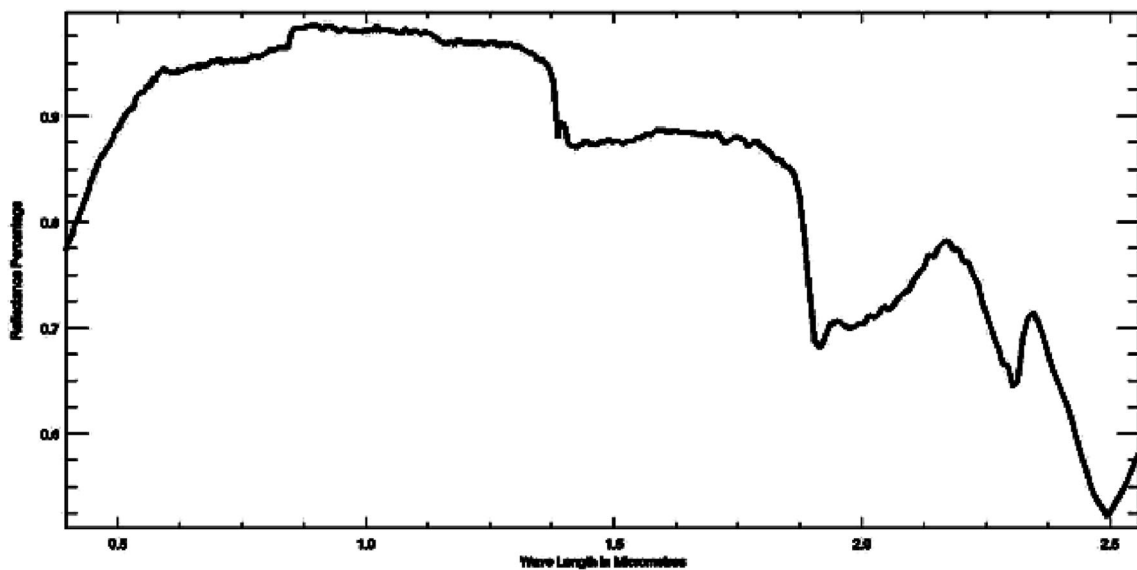


Fig. 15 USGS spectral library plot for magnesite ore mineral

Fig. 16 Lab spectra for peridotite. (i) Hand specimen and respective powdered samples with different grain sizes (250–420 μm , 150–250 μm , 105–150 μm , 63–105 μm , and 37–63 μm). (ii) Reflectance spectra of peridotite for hand specimen and various grain sizes

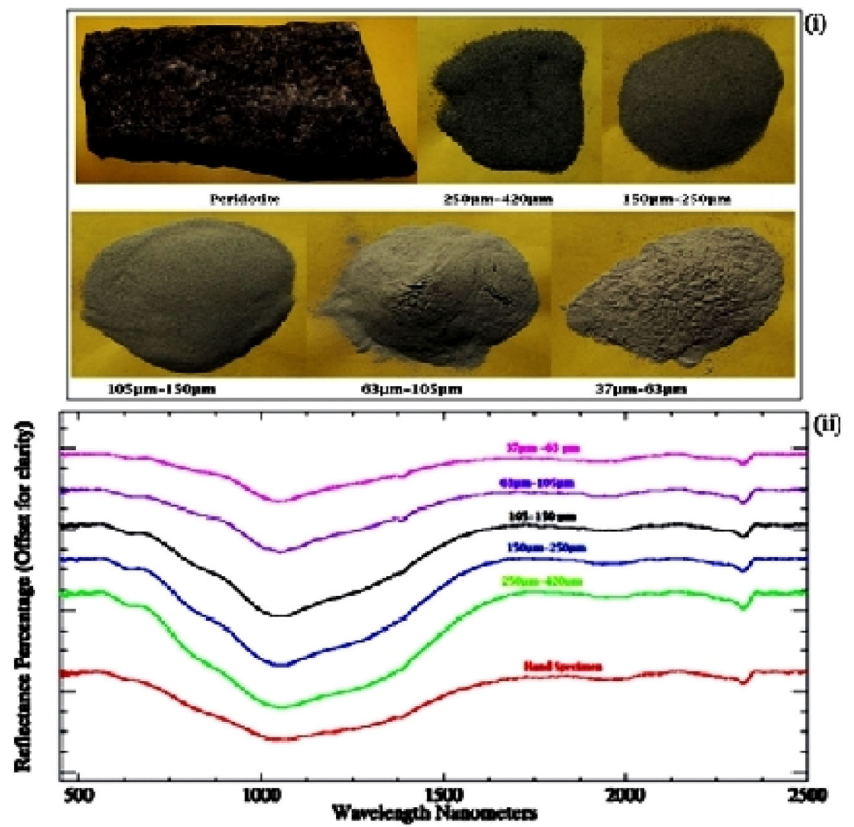


Fig. 17 Lab spectra for dunite. (i) Hand specimen and respective powdered samples with different grain sizes (250–420 μm , 150–250 μm , 105–150 μm , 63–105 μm , and 37–63 μm). (ii) Reflectance spectra of dunite for hand specimen and various grain sizes

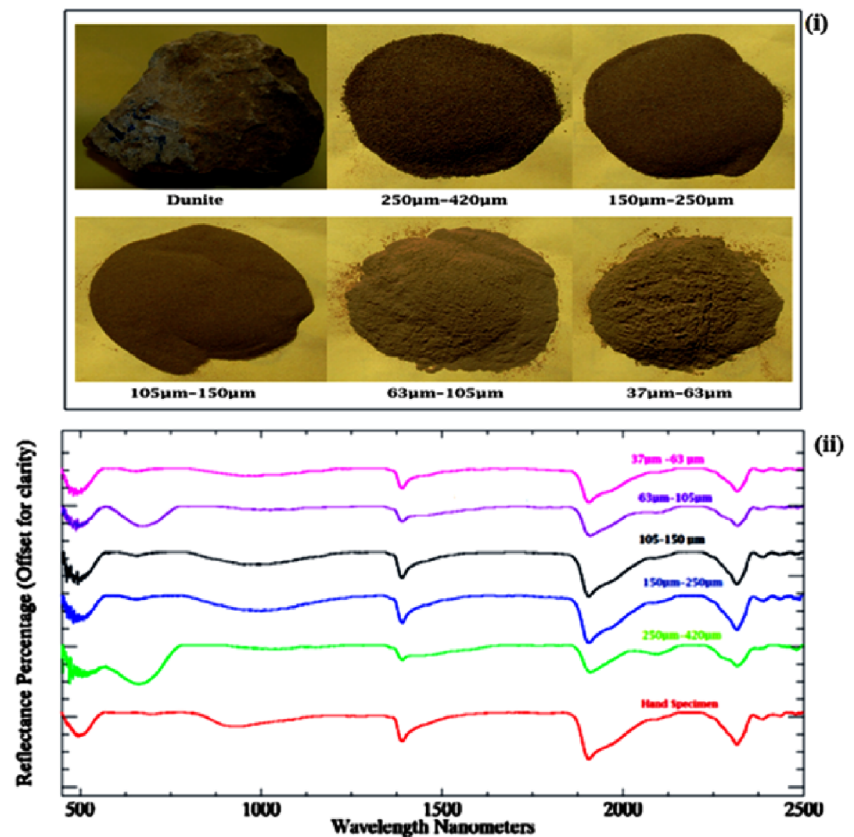


Fig. 18 Lab spectra for weathered dunite. (i) Hand specimen and respective powdered samples with different grain sizes (250–420 μm , 150–250 μm , 105–150 μm , 63–105 μm , and 37–63 μm). (ii) Reflectance spectra of weathered dunite for hand specimen and various grain sizes

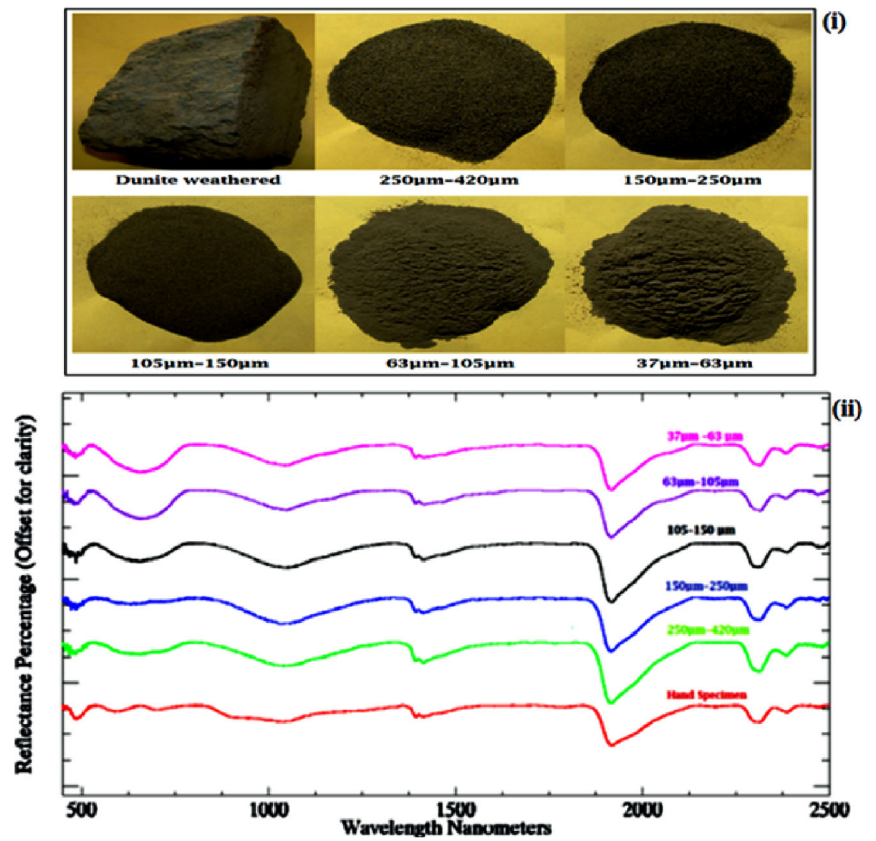


Fig. 19 Lab spectra for siliceous iron dunite. (i) Hand specimen and respective powdered samples with different grain sizes (250–420 μm , 150–250 μm , 105–150 μm , 63–105 μm , and 37–63 μm). (ii) Reflectance spectra of siliceous iron dunite for hand specimen and various grain sizes

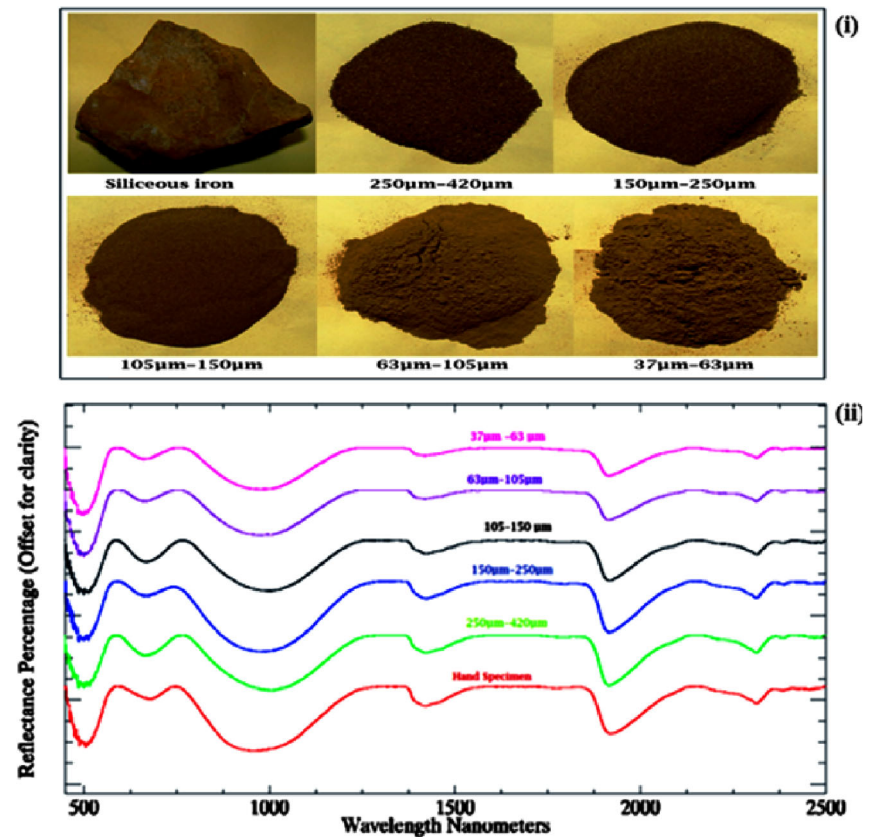
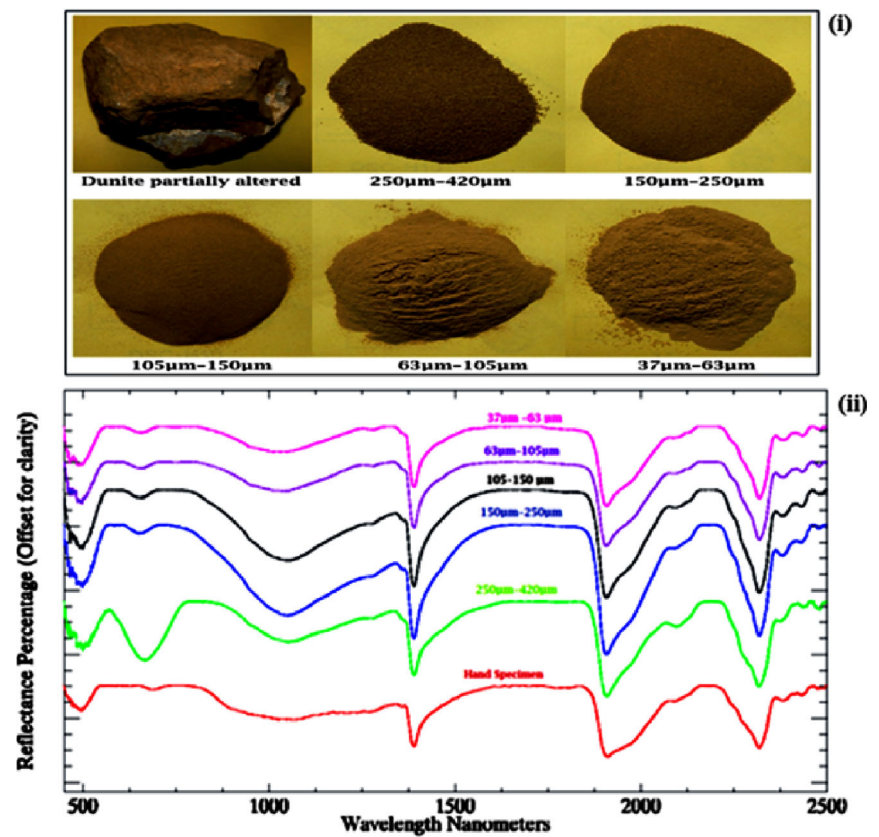


Fig. 20 Lab spectra for partially altered dunite. (i) Hand specimen and respective powdered samples with different grain sizes (250–420 μm , 150–250 μm , 105–150 μm , 63–105 μm , and 37–63 μm). (ii) Reflectance spectra of partially altered dunite for hand specimen and various grain sizes



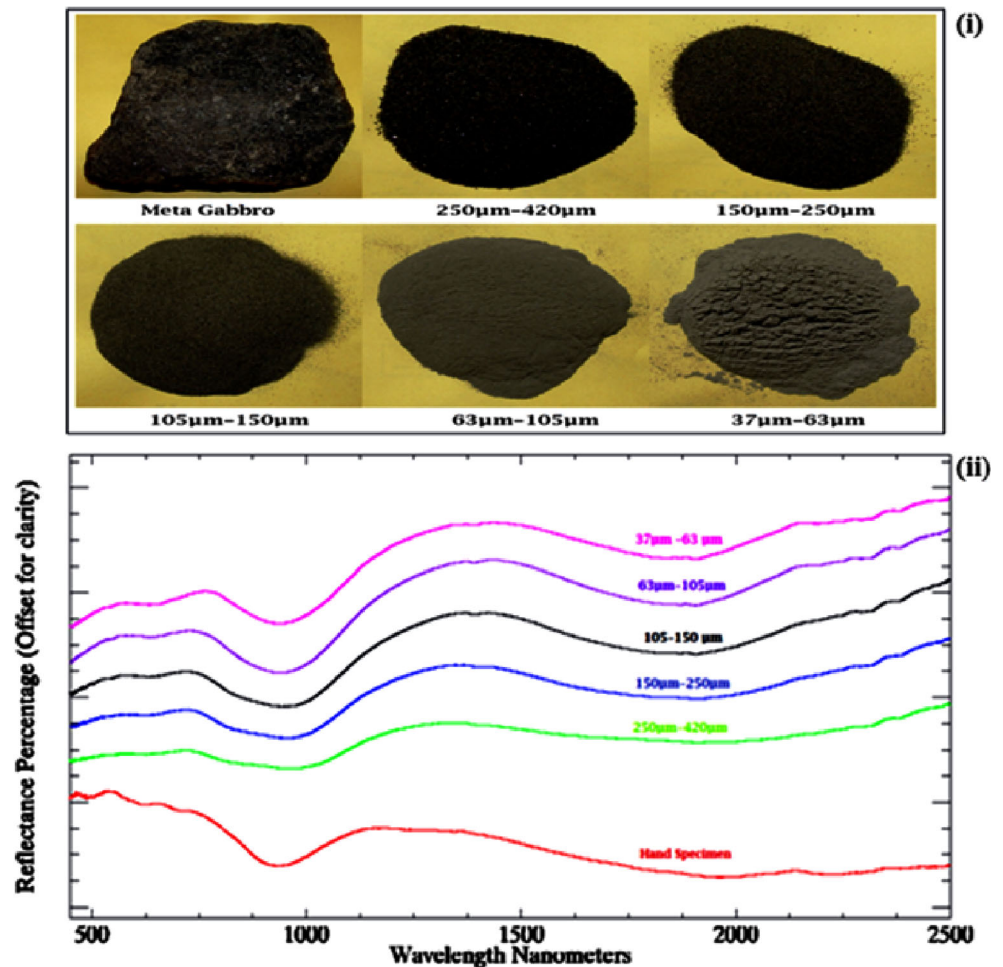
The medium-quality magnesite ore mineral shows the reflectance percentage in the range of 41–90%. Comparatively, the percentage of albedo reduced from 96% for high grade to 90%, medium grade, which indicates the variation in percentage of magnesium content in the ore mineral. Similar to the previous case, absorption features noticed at 1421 nm, 1910 nm, 2310 nm and weak doublets at 2386–2455 nm represent the presence of magnesium and carbonate. The absorption depth in the medium quality is relatively low and weak doublets at 2386–2455 nm represent the moderate percentage of magnesium and carbonate (Fig. 10). The low-grade magnesite sample has reflectance of 30–90%. It has similar absorptions bands as in the prior samples. However, the absorption band depths are not so significant at 1955 nm, 2297 nm, and 2452 nm, which indicate the quality of magnesite and the percentage of magnesium content in the sample. The absorption bands in low-grade magnesite slightly show symmetrical absorption when compared to high-grade minerals (Fig. 11). It also indirectly indicates the low-grade magnesite has a high percentage of silica content. The magnesite sample coated with siliceous iron has the spectral range of 20–80%. Though the sample enriched with magnesium carbonate, the presence of siliceous iron reduces the overall albedo of the reflectance. The presence of iron and olivine represents absorptions at 665 nm and 995 nm. The dominant of hydroxyl ion absorptions in the SWIR region indicates the alteration of

dunite into magnesite ore (Fig. 12). In comparison to other magnesite samples, this sample has strong absorptions at 1966 nm and 2300 nm. Moderate sharp symmetrical absorption noticed at 2455 nm. The above three combinations of absorption bands indicates the presence of MgCO_3 combination. In low grade as well as siliceous iron magnesite ore mineral absorption features at 1420 nm ranges mostly absent in spectral feature. The hydroxyl absorption features may be eliminated due to loss of water / OH molecules in the samples.

In the process of alteration, at few places magnesite is associated with asbestos. The mass of very fine fibers of asbestos associated with magnesite ore appears as dull luster. The altered magnesite ore mineral collected from Dalmia magnesite mines provide moderate absorption bands located at 1393 nm, 1911 nm, and 2321 nm. The VNIR absorptions are absent in the spectra. The albedo ranges from 30 to 63%, which is much lower than the rest of the magnesite ore samples collected from the ultramafic terrain (Fig. 13).

The low albedo and moderate absorption depth indicate low-grade magnesite ore mineral and the percentage of magnesium is also less, which is inferred from chemical analysis. Moreover, the absorptions are mostly matching spectra of actinolite and tremolite asbestos minerals. The spectral reflectance of magnesite sample collected from gossan outcrop is fall in the range of 40–70%. The albedo has once again low when compared to high-grade magnesite ore minerals. The

Fig. 21 Lab spectra for metagabbro. (i) Hand specimen and respective powdered samples with different grain sizes (250–420 μm , 150–250 μm , 105–150 μm , 63–105 μm , and 37–63 μm). (ii) Reflectance spectra of metagabbro for hand specimen and various grain sizes



VNIR spectra of sample are mostly featureless except with very weak absorption at 488 nm (Fig. 14).

Three prominent absorption features for comparisons the spectra of magnesite ore minerals from USGS spectral library noticed at 1420 nm, 1916 nm, and 2300 nm for magnesite

mineral. In addition, two weak absorptions are noticed at 638 nm and 2457 nm (Fig. 15).

Table 4 PCA significant factors of geochemical elements

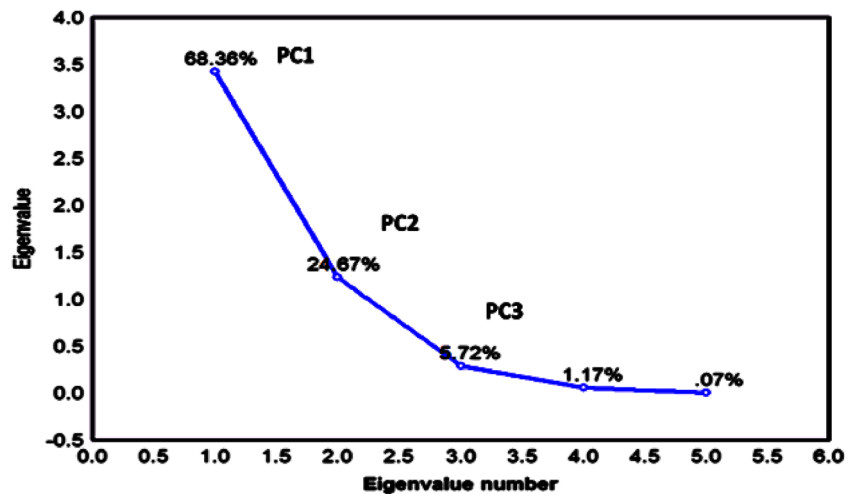
	PCA 1	PCA 2	PCA 3
SiO ₂	-0.953587	0.220997	0.045783
TiO ₂	-0.677310	-0.619299	-0.397117
Al ₂ O ₃	-0.545491	-0.759473	0.353836
MnO	-0.946506	0.299074	0.001841
Fe ₂ O ₃	-0.925506	0.367288	0.033016
CaO	-0.691010	-0.437985	-0.528453
MgO	0.793730	-0.168274	0.369472
Na ₂ O	-0.648306	-0.578865	-0.465179
K ₂ O	-0.430204	-0.557829	0.458048
P ₂ O ₅	-0.867236	-0.385133	-0.143559

Spectra of peridotite and dunite

Peridotite is a dense, fine grained igneous rock, consisting mostly olivine and pyroxene minerals. It is an ultramafic rock containing less than 45% of silica. The carbonate metasomatism of peridotite produced magnesite ore minerals. Spectral measurements were carried out in the laboratory from the peridotite hand specimen and powdered samples. Peridotite has reflectance albedo of 10–50% (Fig. 16). The albedo increases with decreases of particle size, and very slight shifting in band positions. Peridotite has shown prominent, broad absorption feature >1000 nm. It clearly represents in all grain sizes. However, the absorption band depth decreases with decreases of grain sizes. A small symmetrical absorption noticed at 2400 nm.

Dunite is a green color, fine grained igneous rock largely consisting of olivine. The rock sample provides reflectance spectra a range of 10–47%. The absorption features are

Fig. 22 Scree plots of geochemical elements in ore minerals and ultramafic rocks



noticed at 500 nm, 665 nm, 1000 nm, 1392 nm, 1910 nm, 2100 nm, 2316 nm, and 2388–2435nm (Fig. 17). The brownish fine-grained dunite weathered sample collected along the shear zone has a reflectance percentage of 11–55%. The absorption features of weathered dunite are of an almost similar pattern with fresh dunite sample. However, the depth of absorption varies due to alteration in the presence of hydroxyl and carbonate elements (Fig. 18).

The siliceous iron-coated dunite sample represents brownish red color coating, oxidized and enriched with iron siliceous alteration and it has a reflectance percentage of 5–67%. The reflectance spectra of this dunite sample provide clear diagnostic absorption features at 500 nm, 667 nm, 1000 nm, 1425 nm, 1916 nm, and 2315 nm. The presence of olivine as major constituent in the rocks provides well defined broad absorption at 1000nm (Fig. 19). The dunite rock partially altered into magnesite ore minerals in the form of veins. The reflectance spectra obtained in the spectral range of 500–2500nm are plotted as a reflectance percentage after continuum removal.

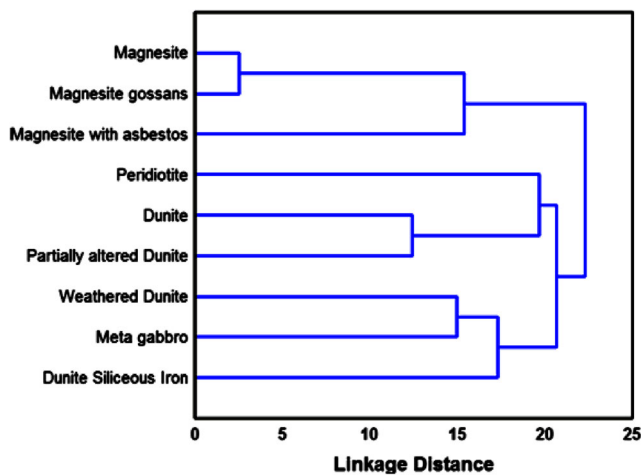


Fig. 23 Cluster analysis dendrogram showing the geochemical elements of ore mineral magnesite and ultramafic rocks

There are eight prominent absorption bands noticed in the plot. The reflectance spectra have shown diagnostic absorption features in the presence of olivine and magnesium carbonate mineral (Fig. 20). The altered dunite prominently shows VIS, NIR, and SWIR spectral absorption due to conversion of silicate dominant composition to carbonate dominant mineral composition (Satish Kumar et al. 2011). The carbonate bands in the SWIR occur at 1900 nm, 2350 nm, and 2550 nm produced due to combinations and overtones confirmed by the diagnosis of carbonates (Gupta 2005).

Spectra of metagabbro

The metagabbro is metamorphosed gabbroic igneous rock consisting of pyroxene, plagioclase feldspar and trace amount of olivine. The percentage of reflectance in metagabbro is 8 to 54%. The meta gabbro show clear, broad absorptions at 950 to 1000 nm due to overlapping component due to pyroxene and olivine, also broad absorption at 1900 nm (Fig. 21). The strong symmetrical absorption at 974 nm and broad, strong absorption at 1911 nm, respectively indicates presence of high calcic pyroxene and ferrous ion in orthopyroxene.

PCA and cluster analysis

The principal component analysis applied to the geochemistry data obtained from the XRF analysis reveals that the correlated variables in a numerical approach either positive or negative values. The variables of the samples are assumed to lie on the linear composition. The pearson’s correlation generally measures the strength of two variables in a linear relationship. The correlation value represents positive correlation shown as bold in Table 3. The MgO component’s correlation values show a negative except with MgO combination indicating a non-correlation with other variables.

The variables mainly combine with the other variable combination to obtain the PCA1, PCA2, and PCA3 values

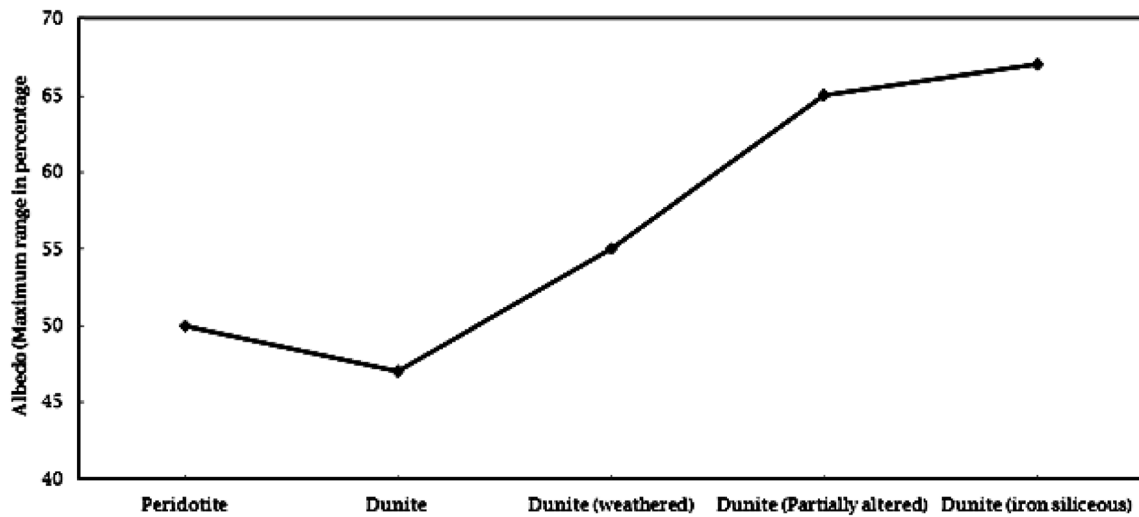


Fig. 24 Percentage of albedo in various ultramafic rocks

(Table 4). The component data sets used for major oxides were utilized to find the PCA variance that reflects a high score in PC1 (68.36%), PC2 (24.67%), and PC3 (5.72%) with respect to eigen values and eigen number (Fig. 22).

PCA loadings (90% of the total variance) and scores in scree plots exhibited the grouping and relationship between the magnesite ore minerals and ultramafic rocks which signified the strength of their mutual relation. By cluster analysis, group 1 represents magnesite ore minerals such as magnesite, magnesite gossan and magnesite with asbestos. On the other hand, group 2 clearly represents ultramafic rocks such as peridotite, dunite and altered dunite. Lastly, group 3 represents weathered dunite, dunite with siliceous iron and metagabbro. Hence, it is noticed that group 1 components are highly correlated to each other with high concentration of MgO. However, Group 2 and Group 3 indicate medium to low concentration of MgO due to alteration of rocks. Consider the PCA scree plot with PC1 and PC2 have exactly the same grouping as the cluster analysis (Fig. 23).

Conclusion

Reflectance spectral measurements were carried out for magnesite ore minerals and rock samples collected from Salem ultramafic terrain. Out of various rock types, peridotite and dunites are considered as the significant in the spectral studies, since these are host rock for magnesite ore mineral deposits. The petrographical study has indicated that the presence of olivine as the major mineral in the parent rocks such as peridotite and dunite. The other minerals identified in the thin sections are pyroxene, chromite and mafic minerals. Olivine is the major mineral in most of the rocks, which reflects in the spectra as broad absorptions mostly at 1050nm. The common absorption bands in the dunite are 640 nm, 1050 nm, 1392 nm, 1910 nm, 2325 nm, and 2388 nm. These respective bands indicate the presence of ferric iron, olivine pyroxene overlapping, OH/Mn³⁺, OH/Fe²⁺, Mg-OH vibration and carbonate absorptions. The increase of percentage of particular elements usually increases the absorption strength and shifting of band

Fig. 25 Albedo in varieties of magnesite ore minerals

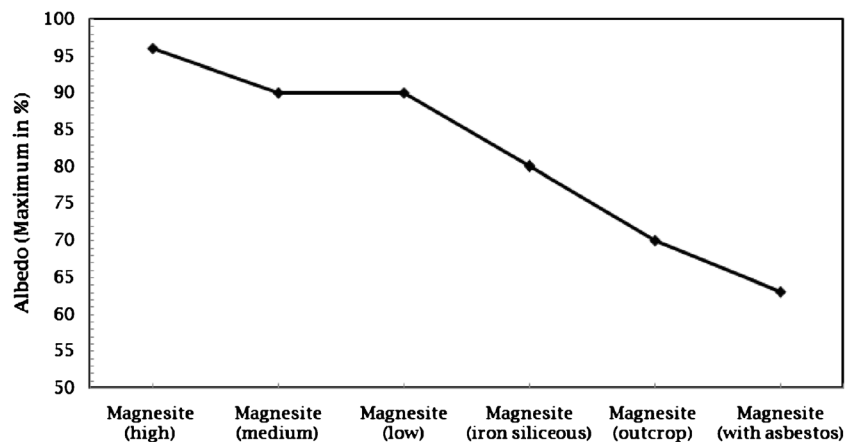


Table 5 Laboratory spectral observation of magnesite ore mineral and absorption band characteristics

Ore minerals	1900 nm	2300 nm	2450 nm
Magnesite high grade	Strong asymmetry	Moderate left shoulder	Weak symmetrical
Magnesite medium grade	Strong asymmetry	Moderate asymmetrical weak shoulder	Weak doublets
Magnesite low grade	Moderate symmetry	Moderate symmetrical	Weak
Magnesite siliceous iron	Strong right shoulder	Very strong symmetry	Moderate symmetry
Magnesite with asbestos	Moderate asymmetry right shoulder	Moderate asymmetry left shoulder	Very weak
Magnesite gossan	Weak asymmetry	Weak symmetry	Very weak symmetry

centers. The albedo directly proportional to the altered condition of the ultramafic rocks, that is, the fresh rock has less albedo than the altered rock samples (Fig. 24).

The magnesite ore minerals clearly depict that the increasing degree of alteration that SiO₂ can replace with magnesium carbonates subsequently fully altered into magnesite. These trends of alteration clearly depict in geochemistry and spectral behavior of different kinds of magnesite ore minerals. The fully altered high-grade magnesite ore minerals show diagnostic spectral characteristics with maximum albedo of 96%. It has absorption features at 1420 nm, 1916 nm, 2300 nm, and doublets at 2390–2457nm.

In the VNIR portion, it shows a rise in albedo in convex reflectance pattern. In most cases, the combination of above absorption features indicates magnesium carbonate in the composition. The quality of ore minerals and the presence of MgCO₃, silica and iron content influence the albedo percentage. The high-grade magnesite with less amount of silica content has high albedo in the spectral plot (Fig. 25).

The absorption band depths for hand specimen and powdered samples were calculated for the diagnosis of absorption bands in the spectra of various magnesite minerals. The average of all values is considered as final absorption depth value for respective bands. The presences of 1900 nm, 2300 nm, and 2500 nm absorption bands in the spectra are the diagnostic spectra of magnesite ore minerals. The absorption depth 0.07 and 0.31 respectively obtained for low and medium quality magnesite ore minerals at 1900 nm. Similarly, at 2300 nm low grade have 0.15 and magnesite with asbestos have 0.25 absorption depths. However, further detailed assessment is

required along with more number of samples and chemical data. The spectral characteristics of various magnesite ore minerals are listed in Table 5. Though the characteristics do not show any definite trend for quality of ore minerals, the strong to moderate absorption noticed at 1900 nm for quality and grade of minerals and weak to very weak absorption noticed for the rest of the minerals.

The presence of silicates, magnesium oxides and ferrous oxides and their percentage determined the quality of rocks being utilized for industrial purpose. The percentage of silicate is the major parameter which controls grade of ore minerals. Hence, the three major oxides were categorized from chemical analysis (Table 6) and also computed in the PCA scores with variable PCA1 that indicates the association with other variable which provide MgO concentration with positive and high score (Table 4).

The range of major oxides present in the host rocks like peridotite and dunite of magnesite indicates the quality of rock that suits for commercial purposes (Table 7). From the above analysis, it is clearly understood that when SiO₂ percentage increases, the MgO percentage decreases, particularly in weathered dunite and iron siliceous rich dunite samples. On the other hand, when MgO percentage increases SiO₂ percentage decreases in the samples of peridotite, dunite and partially altered dunite samples. The same relationship is noticed between Fe₂O₃ and MgO. XRF analyses were obtained for medium grade, partially altered magnesite and outcrop sample. The quality of magnesite once again determined by

Table 6 Categorization of chief major oxides in ore minerals

Category	SiO ₂ %	MgO%	Fe ₂ O ₃ %
High	<40%	>50%	<10%
Moderate	30-40%	40-50%	5-8%
Low	>45%	<25%	>9%

Table 7 Chief major oxides in ultramafic rocks

Sample	SiO ₂ %	MgO%	Fe ₂ O ₃ %
Peridotite	low	high	low
Dunite	low	moderate	low
Dunite Weathered	moderate	low	moderate
Dunite Siliceous iron	high	low	high
Partially altered Dunite	low	moderate	low

the percentage of silicate present in the ore minerals. The percentage of MgO presents in the samples, respectively 41.06%, 35.25%, and 41.56%. The silicate percentage is 10.49%, 22.25%, and 9.7%. The integrated results of spectral studies, mineralogy, and geochemistry comply with the quality of magnesite ore minerals and ultramafic rocks.

Acknowledgements The authors thank to SAIL refractory, TANMAG and Dalmia Magnesite mines for providing permission to collect samples. Essen & Co, Salem extended support for pulverizing the samples. Thin section prepared at Department of Geology, University of Kerala. Spectral measurement was carried out at IIST-ISRO, Trivandrum and XRF analysis carried out at NCESS, Trivandrum. The first author thanks University Grants Commission (UGC) for providing BSR fellowship.

Declarations I declared that the manuscript is the authors' original work and the manuscript has not received prior publication and is not under consideration for publication elsewhere.

Conflict of interest The authors declare that they have no competing interests.

References

- Anbazhagan S, Arivazhagan S (2010) Reflectance spectra of analog anorthosites: Implications for lunar highland mapping. *Planetary and Space Science*, Elsevier, No. 58:752–760
- Anbazhagan S, Arivazhagan S (2009) Reflectance spectra of analog basalts; implications for remote sensing of lunar geology. *Planetary and Space Science*, Elsevier, No. 58:1346–1358
- Bailin Y, Xingli W (1991) Spectral reflectance features of rocks and ores and their Applications. *Chinese Journal of Geochemistry* 10(2):188–195
- Brouwer PN (2010) *Theory of XRF*. Third edition, PANalytical BV, The Netherlands. ISBN: 90-9016758-7, p.58
- Chen S, Grunsky EC, Hattori K, Liu Y (2015) Principal Component Analysis of Geochemical Data from the REE-rich Maw Zone, Athabasca Basin. Canada; Geological Survey of Canada, Open File 7689:24p. <https://doi.org/10.4095/295615>
- Chetty TRK (1996) Proterozoic shear zones in Southern Granulite Terrain, India. *Gond.Res. Group Mem.3: The Archaean and Proterozoic terranes in Southern India within East Gondwana*, pp.77-90
- Chung SY, Venkatramanan S, Park N, Rajesh R, Ramkumar T, Kim BW (2015) An assessment of selected hydrochemical parameter trend of the Nakdong River water in South Korea, using time series analyses and PCA. *Environ Monit Assess*, Springer, Vol. 187(4):1–13
- Chung SY, Venkatramanan S, Park NN, Ramkumar T, Sujitha SB, Jonathan MP (2016) Evaluation of physico-chemical parameters in water and total heavy metals in sediments at Nakdong River Basin, Korea. *Environmental Earth Sciences*. Springer, pp 75–50
- Chung B, Yu J, Wang L, Kim NH, Lee BH, Koh S, Lee S (2020) Detection of Magnesite and Associated Gangue Minerals using Hyperspectral Remote Sensing—A Laboratory Approach. *Remote Sens*. Vol. 12:1325. <https://doi.org/10.3390/rs12081325>
- Clark RN, Gallagher AJ, Swayze GA (1990) Material Absorption Band Depth Mapping of Imaging Spectrometer Data Using a Complete Band Shape Least-Squares Fit with Library Reference Spectra. In: *Proceedings of the Second Airborne Visible/Infrared Imaging Spectrometer (AVIRIS) Workshop*. JPL Publication 90-54, pp 176–186
- Clark RN (1999) *Spectroscopy of Rocks and Minerals, and Principles of Spectroscopy*. In: Rencz AN (ed) *Manual of Remote Sensing*, Vol. 3, *Remote Sensing for the Earth Sciences*. John Wiley and Sons, New York, pp 3–58
- Friend CRL, Janardhan AS (1984) Mineral chemistry of coexisting phases from shonkinitic rocks, Salem, Tamil Nadu, India. *Mineralogical Magazine*, VOL. 48, pp. 181–193
- Gadsden, Aric JA (1975). *Infrared spectra of minerals and related inorganic compounds*, First Edition, Butterworths group & Co (Publisher), England, p. 271
- Gaffey SJ (1986) Spectral reflectance of carbonate minerals in the visible and near infrared (0.35–2.55 microns): calcite, aragonite, and dolomite. *American Mineralogist* 71:151–162
- Gazley M F, Collins K S, Roberston J, Hines B R, Fisher L.A and Mc Farlane A (2015). Application of principal component analysis and cluster analysis to mineral exploration and mine geology , Aus IMM New Zealand Branch Annual Conference 2015, pp131-139
- Geological Survey of India (GSI) (2006) *Geology and Mineral Resources of the states of India*. Miscellaneous Publication, Part VI - Tamil Nadu and Pondicherry, pp.:1–59
- Gupta RP (2005) *Remote Sensing Geology*, 2nd edn. Springer verlag, Berlin, p 627
- He XF, Santosh M, Zhang ZM, Tsunogae T, Chetty TRK, Ram Mohan M, Anbazhagan S (2015) Shonkinites from Salem, southern India: Implications for Cryogenian alkaline magmatism in rift-related setting. *Journal of Asian Earth Sciences*, Elsevier (113):812–825
- Madani AA (2011) Spectral properties of carbonatized ultramafic mantle xenoliths and their host olivine basalts, Jabal Al Maqatl basin, South Eastern Desert, Egypt, using ASD FieldSpec spectroradiometer. *The Egyptian Journal of Remote Sensing and Space Sciences*, Elsevier 14:41–48
- Murthy SRN (1979) *Records of Geological Survey of India* 112(5):15–35
- Mustard JF, Pieters CM (1987) Abundance and Distribution of Ultramafic Microbreccia in Moses Rock Dike: Quantitative Application of Mapping Spectroscopy. *Journal of Geophysical Research* 92(B10):376–390
- Paramasivam CR (2016) *Remote sensing and spectral studies of magnesite mining area, Salem, India*. Ph.D Thesis, Periyar University, Periyar Palkalai Nagar, Salem, Tamil Nadu, India, 193 pp.
- Petruk W (2000) *Applied mineralogy in the mining industry*, 1st edn. Elsevier (Publisher), The Netherlands, p 268
- Raith MM, Raase P, Reinhardt J (2011) *Guide to Thin Section microscopy*. second edition, ISBN : 978-3-00-033606-5 (PDF), p.107
- Satish Kumar J, Sanjeevi S, Govindan S (2011) Hyperspectral Radiometry to Characterise Dunite Alteration and Magnesite Deposits of Salem, South India. *Journal of Indian Society Remote Sensing*, Springer (39 (4)):497–505
- Tellen VA, Yerima BPK (2018) Effects of land use change on soil physicochemical properties in selected areas in the North West region of Cameroon. *Environmental Systems Research*, Springer:1–29. <https://doi.org/10.1186/s40068-018-0106-0>
- Van der Meer F, De Jong S (2003) Spectral mapping methods: many problems, some solutions. In: *3rd EARSeL Workshop on Imaging Spectroscopy*, Hirsching, pp 146–162
- Verma PK (2010) *Optical mineralogy*. Ane Books Pvt. Ltd (Publisher), New Delhi, p 369
- Xue J, Lee C, Wakeham SG, Armstrong RA (2011) Using principal components analysis (PCA) with cluster analysis to study the organic geochemistry of sinking particles in the ocean. *Organic Geochemistry*, Elsevier 42:356–367
- Zadeh MH, Tangestani MH, Roldan FV, Yusta I (2014) Spectral characteristics of minerals in alteration zones associated with porphyry copper deposits in the middle part of Kerman copper belt, SE Iran. *Ore Geology Reviews*, Elsevier (62):191–198